Cell-specific discrimination of desmosterol and desmosterol mimetics confers selective regulation of LXR and SREBP in macrophages

Evan D. Muse[a,b,1], Shan Yu[c,1], Chantle R. Edillor[a,2], Jenhan Tao[a,2], Nathanael J. Spann[a], Ty D. Troutman[a], Jason S. Seidman[a], Adam Henke[c], Jason T. Roland[c], Katherine A. Ozeki[a], Bonne M. Thompson[d], Jeffrey G. McDonald[d], John Bahadorani[e], Sotirios Tsimikas[e], Tamar R. Grossman[f], Matthew S. Tremblay[c,3], and Christopher K. Glass[a,e,3,4]

[a]Department of Cellular and Molecular Medicine, School of Medicine, University of California, San Diego, La Jolla, CA 92093; [b]Division of Cardiovascular Diseases, Scripps Clinic, Scripps Translational Science Institute, La Jolla, CA 92037; [c]California Institute for Biomedical Research, La Jolla, CA 92037; [d]Center for Human Nutrition, University of Texas Southwestern Medical Center, Dallas, TX 75390; [e]Department of Medicine, University of California, San Diego, La Jolla, CA 92093; and [f]Ionis Pharmaceuticals, Carlsbad, CA 92010

Contributed by Christopher K. Glass, March 14, 2018 (sent for review August 23, 2017; reviewed by Steven J. Bensinger and Carlos Fernandez-Hernando)

Activation of liver X receptors (LXRs) with synthetic agonists promotes reverse cholesterol transport and protects against atherosclerosis in mouse models. Most synthetic LXR agonists also cause marked hypertriglyceridemia by inducing the expression of sterol regulatory element-binding protein (SREBP)1c and downstream genes that drive fatty acid biosynthesis. Recent studies demonstrated that desmosterol, an intermediate in the cholesterol biosynthetic pathway that suppresses SREBP processing by binding to SCAP, also binds and activates LXRs and is the most abundant LXR ligand in macrophage foam cells. Here we explore the potential of increasing endogenous desmosterol production or mimicking its activity as a means of inducing LXR activity while simultaneously suppressing SREBP1c-induced hypertriglyceridemia. Unexpectedly, while desmosterol strongly activated LXR target genes and suppressed SREBP pathways in mouse and human macrophages, it had almost no activity in mouse or human hepatocytes in vitro. We further demonstrate that sterol-based selective modulators of LXRs have biochemical and transcriptional properties predicted of desmosterol mimetics and selectively regulate LXR function in macrophages in vitro and in vivo. These studies thereby reveal cell-specific discrimination of endogenous and synthetic regulators of LXRs and SREBPs, providing a molecular basis for dissociation of LXR functions in macrophages from those in the liver that lead to hypertriglyceridemia.

macrophage | LXR | hepatocyte | cholesterol | SREBP

Although improvements in the prevention and treatment of cardiovascular disease (CVD) over the last decade have contributed to a significant reduction in the burden of CVD, it still accounts for nearly a third of all deaths in the United States and worldwide each year (1). In fact, more people die each year secondary to CVD than any other cause, with coronary heart disease and stroke representing the majority of cases (2). Increased apolipoprotein B-100–associated lipid species, namely LDL cholesterol (LDL-C), remains one of the best-appreciated risk factors for atherosclerotic heart disease. Accordingly, reduction of LDL-C through the use of statins or recently developed antibodies directed against proprotein convertase subtilisin/kexin type 9 represents one of the mainstays of preventive therapy (3, 4). However, myocardial infarction and stroke still occur in a subset of individuals despite cholesterol lowering, and therapies directed at additional targets are of potential clinical benefit.

Macrophages are key cellular players in the initiation and progression of atherosclerosis through their roles in uptake of modified lipoproteins in the artery wall, production of inflammatory mediators, and secretion of metalloproteases that contribute to plaque instability (5–8). A subset of macrophages within atherosclerotic lesions are characterized by massive accumulation of cholesterol esters in lipid droplets, resulting in a "foam cell" phenotype indicative of a failure of normal cholesterol homeostasis. Given their central role in integrating both cholesterol homeostasis and inflammatory signaling in macrophages, the liver X receptors (LXRs) represent logical targets for pharmacologic intervention in atherosclerosis (9–11). LXR activation is known to promote cholesterol efflux in macrophages by activation of ATP-binding cassette transporter A1 and G1 (ABCA1/ABCG1) (12, 13) while also repressing the proinflammatory products of NF-κB signaling (14). Stimulation of cholesterol efflux in macrophages and other cell types contributes to overall functions of LXRs in mediating reverse cholesterol transport from peripheral cells to the liver for biliary secretion (15, 16).

Consistent with these homeostatic functions, deletion of LXRs either at the whole-body level or within the hematopoietic

Significance

The beneficial effects of LXR-pathway activation have long been appreciated, but clinical application of synthetic LXR ligands has been limited by coactivation of SREBP1c and consequent hypertriglyceridemia. Natural LXR ligands such as desmosterol do not promote hypertriglyceridemia because of coordinate down-regulation of the SREBP pathway. Here we demonstrate that synthetic desmosterol mimetics activate LXR in macrophages both in vitro and in vivo while suppressing SREBP target genes. Unexpectedly, desmosterol and synthetic desmosterol mimetics have almost no effect on LXR activity in hepatocytes in comparison with conventional synthetic LXR ligands. These findings reveal cell-specific differences in LXR responses to natural and synthetic ligands in macrophages and liver cells that provide a conceptually new basis for future drug development.

Author contributions: E.D.M., S.Y., C.R.E., N.J.S., T.D.T., J.S.S., A.H., J.T.R., K.A.O., J.G.M., S.T., T.R.G., M.S.T., and C.K.G. designed research; E.D.M., S.Y., C.R.E., N.J.S., T.D.T., J.S.S., A.H., J.T.R., K.A.O., B.M.T., J.G.M., and J.B. performed research; A.H., J.T.R., J.B., S.T., and T.R.G. contributed new reagents/analytic tools; E.D.M., S.Y., C.R.E., J.T., N.J.S., T.D.T., J.S.S., K.A.O., B.M.T., J.G.M., S.T., M.S.T., and C.K.G. analyzed data; and E.D.M., S.Y., M.S.T., and C.K.G. wrote the paper.

Reviewers: S.J.B., University of California, Los Angeles; and C.F.-H., Yale University School of Medicine.

The authors declare no conflict of interest.

Data deposition: Sequencing data supporting these studies have been deposited in the Gene Expression Omnibus (GEO) database, https://www.ncbi.nlm.nih.gov/geo (accession no. GSE90615).

See Commentary on page 5051.

[1]E.D.M. and S.Y. contributed equally to this work.

[2]C.R.E. and J.T. contributed equally to this work.

[3]M.S.T. and C.K.G. contributed equally to this work.

[4]To whom correspondence should be addressed. Email: ckg@ucsd.edu.

This article contains supporting information online at www.pnas.org/lookup/suppl/doi:10.1073/pnas.1714518115/-/DCSupplemental.

Published online April 9, 2018.

compartment results in accelerated atherosclerosis in mouse models (17, 18). Conversely, administration of potent synthetic LXR agonists, such as GW3965, inhibits the development of atherosclerosis in these models (19–21). However, most synthetic agonists of LXR have also been found to strongly activate sterol regulatory element-binding protein (SREBP)1c and downstream genes involved in fatty acid biosynthesis, including fatty acid synthase (FAS), that subsequently lead to increased serum cholesterol and triglyceride levels (22, 23). Thus, while activating LXR has positive effects in the prevention of atherosclerosis in terms of enhancing reverse cholesterol transport and suppression of proinflammatory pathways, the negative aspect of hypertriglyceridemia and fatty liver—a product of SREBP activation—has prevented synthetic LXR agonists from being clinically useful therapeutics. Empiric efforts to develop "dissociated" LXR agonists that retain the ability to activate LXRs but do not induce hypertriglyceridemia have been partially successful (24–27), but underlying mechanisms are poorly understood.

LXR activity is normally induced under conditions of cholesterol excess in a manner that is reciprocal to coordinate inhibition of the processing of the SREBP transcription factors. LXRs do not sense cholesterol directly but are instead positively regulated by oxysterols and intermediates in the cholesterol biosynthetic pathway (28–30). In contrast to most synthetic LXR agonists, natural LXR agonists also suppress processing of the SREBP proteins (31). In the case of oxysterols, such as 25-hydroxycholesterol, inhibition is mediated through interactions with the insulin-induced gene (INSIG) proteins that prevent trafficking of SREBPs to the Golgi for proteolytic activation (32). The cholesterol biosynthetic intermediate desmosterol was first noted to be an endogenous LXR-activating ligand in studies of plant sterols and sterol intermediates in the cholesterol biosynthetic pathway (30). In contrast to oxysterols, desmosterol most likely suppresses SREBP processing by interacting with SREBP cleavage-activating protein (SCAP) to retain the SREBPs in the endoplasmic reticulum (31).

In a lipidomic analysis of murine macrophage foam cells and human atherosclerotic plaques, desmosterol was found to be the most abundant endogenous LXR activator (33). The accumulation of desmosterol in macrophage foam cells was correlated with down-regulation of *Dhcr24*, which encodes the 24-dehydroxycholesterol reductase enzyme that converts desmosterol to cholesterol (Fig. 1*A*). Notably, treatment of macrophages with increasing concentrations of desmosterol led to coordinate increases in LXR-dependent pathways and suppression of SREPB pathways. As a consequence, genes involved in cholesterol efflux were induced, while genes involved in cholesterol and fatty acid synthesis were down-regulated (33). These findings confirmed the prediction that desmosterol could balance lipid homeostasis via reciprocal actions on LXR and SREBP activities (30).

These observations raised the questions of whether the desmosterol pathway operates in other cell types and whether it would be possible to activate this pathway, or mimic it, as a therapeutic strategy. Studies in mouse macrophages pointed to down-regulation of *Dhcr24* as being the key event leading to accumulation of desmosterol (33). One straightforward strategy would thus be to inhibit 24-dehydrocholesterol reductase (DHCR24) activity. Remarkably, this was first achieved more than 50 y ago following the identification of triparanol (also known as mer-29) as a potent inhibitor of DHCR24. Administration of triparanol to hypercholesterolemic human subjects led to marked reductions in serum cholesterol and corresponding rises in circulating desmosterol (34, 35). However, triparanol was rapidly withdrawn from the market after reports of severe cataracts and alopecia (36–38), and there is no evidence of whether there was an impact on the development of cardiovascular diseases. While there are dermatologic manifestations of desmosterolosis, it is unknown if the extent of alopecia or development of cataracts is specifically related to increased circulating desmosterol or potentially an off-target effect of triparanol (39).

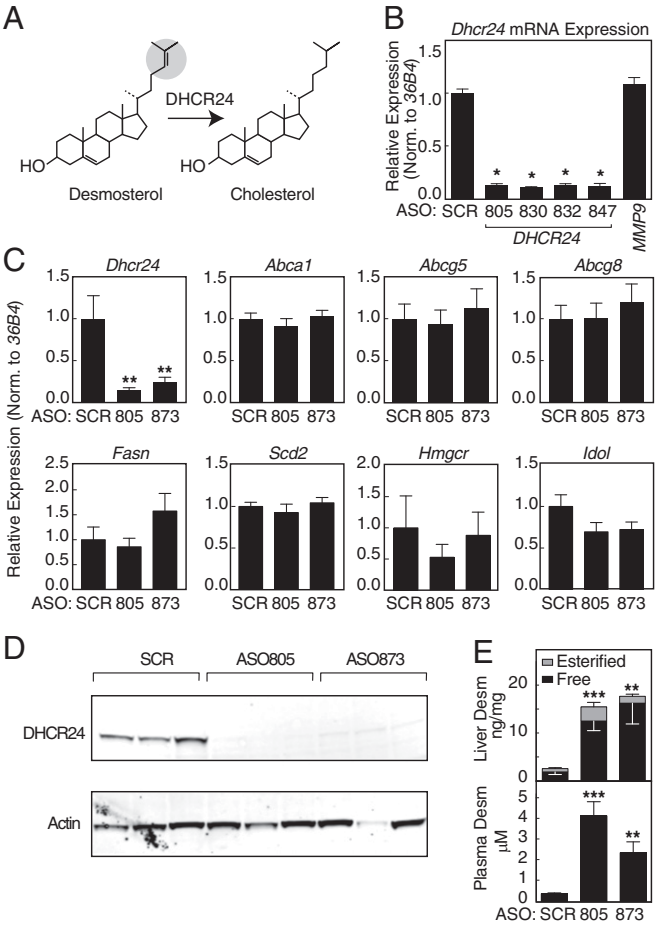

Fig. 1. Effect of 24-dehydrocholesterol reductase-specific antisense oligonucleotide treatment in mice. (*A*) Catalysis of the final step in cholesterol biosynthesis by *Dhcr24*. (*B*) Effect of treatment of mouse thioglycollate-elicited macrophages with four separate ASOs to *Dhcr24* (ION-599805, ION-599830, ION-599832, and ION-599847, hereafter indicated as 805, 830, 832, and 847, respectively) or an ASO directed at *Mmp9* (MMP9 ASO), as assessed by RT-qPCR (*$P < 0.0001$ vs. SCR). (*C*) Gene expression levels of the indicated genes in mouse liver after treatment with ASO (**$P < 0.001$). (*D*) Western immunoblot analysis of Dhcr24 and actin in liver protein extracts in mice treated with the indicated *Dhcr24*-specific ASOs. (*E*) Plasma and liver desmosterol concentrations as measured by LC-MS in mice treated with *Dhcr24*-specific compared with SCR ASOs (**$P < 0.01$, ***$P < 0.001$). Error bars represent standard errors.

Here we investigate the potential to modulate and mimic the desmosterol pathway in vivo and in vitro as a means of coordinately regulating the LXR and SREBP pathways. To modulate the desmosterol pathway in vivo, we developed potent and specific antisense oligonucleotides (ASOs) that reduce *Dhcr24* expression in the liver by more than 80%. Unexpectedly, while this treatment resulted in significant increases in endogenous desmosterol, no significant changes in LXR or SREBP target genes were observed in the liver. To mimic the desmosterol pathway, we demonstrate that the previously reported selective LXR modulators DMHCA (27) and MePipHCA (40) have properties of synthetic desmosterol mimetics. While desmosterol, DMHCA, and MePipHCA coordinately regulate the LXR and SREBP pathways in primary mouse and human macrophages, they exhibit very little effect on gene expression in primary mouse and human hepatocytes. The differential effects of DMHCA and MePipHCA on

LXR and SREBP target genes in macrophages and hepatocytes are also observed in vivo. Remarkably, LXR target genes are activated in Kupffer cells in response to DMHCA, in contrast to liver as a whole. In concert, these findings suggest a molecular basis for dissociation of LXR functions in macrophages and hepatocytes that would enable retention of antiatherogenic properties without promoting hypertriglyceridemia.

Results

Blockade of DHCR24 Using Gene-Specific ASOs Leads to Increased Endogenous Desmosterol Without Potentiating LXR-Mediated Target Genes. To modulate the endogenous desmosterol pathway for coordinate regulation of LXR and SREBP target genes in vivo, we developed ASOs specific to DHCR24. Based on the effects of inhibition of DHCR24 by triparanol and genetic deficiency of *Dhcr24*, we hypothesized that reduction of *Dhcr24* expression would lead to increased desmosterol levels and corresponding changes in LXR- and SREBP-dependent gene expression (Fig. 1*A*). Out of more than 50 potential *Dhcr24*-specific ASOs developed and initially assayed, we tested four of the most active ASOs in plated thioglycollate-elicited macrophages (TGEMs) (Fig. 1*B*). After 48 h of exposure to ASO, *Dhcr24* gene expression as assessed through quantitative real-time PCR (qRT-PCR) was less than a quarter of scramble (SCR) control with four separate *Dhcr24*-specific ASOs (ION-599805, ION-599830, ION-599832, and ION-599847, hereafter referred to as 805, 830, 832, and 847, respectively). *Dhcr24* gene expression was also unchanged by a negative control MMP9 ASO compared with the SCR-treated cells. We then aimed to use these ASOs to reduce *Dhcr24* expression in C57BL/6 mice.

We delivered control (SCR) ASO and the DHCR24-specific ASOs 805 and ION-599873 (referred to as 873) to six mice per group via biweekly i.p. injections over a 3-wk period (Fig. S1*A*). The treatment regimen was well-tolerated in all study groups, with expected weight gain and no difference in body weights at the termination of the study (Fig. S1*B*). Following 3 wk of treatment, hepatic expression of *Dhcr24* was markedly reduced in both cohorts of *Dhcr24* ASO-treated animals compared with SCR control (15 and 25% vs. SCR control for 805 and 873, respectively, $P < 0.001$) (Fig. 1*C*). This was mirrored by a substantial reduction in DHCR24 gene product as examined by Western immunoblot analysis of liver extract (Fig. 1*D*). Concomitant with this reduction of *Dhcr24* gene expression and protein, circulating plasma desmosterol increased by 10-fold after treatment with *Dhcr24* ASO (0.38 ± 0.04, 3.97 ± 0.65, and 2.27 ± 0.50 μM for SCR, 805, and 873, respectively) as measured by liquid chromatography-mass spectrometry (LC-MS) (Fig. 1*E*). In addition, hepatic desmosterol levels increased after *Dhcr24* ASO treatment (1.87 ± 0.53, 12.50 ± 2.01, and 16.23 ± 4.34 ng/mg for SCR, 805, and 873, respectively), attributable mainly to increases in free rather than esterified desmosterol (Fig. 1*E*). Surprisingly, despite these increases in circulating and hepatic desmosterol, there were no observed alterations in the expression of the key hepatic LXR target genes ATP-binding cassette transporter subfamily A, member 1 (*Abac1*), ATP-binding cassette transporter subfamily G, member 5 (*Abcg5*), or ATP-binding cassette transporter subfamily G, member 8 (*Abcg8*) in *Dhcr24* ASO-treated animals versus SCR control (Fig. 1*C*). Nor were there differences in the hepatic expression of SREBP target genes (Fig. 1*C*).

In a second experimental paradigm, we performed 1 wk of s.c. ASO treatment in C57BL/6 mice that received thioglycollate 4 d before study end. Both liver and TGEMs showed a reduction in *Dhcr24* gene expression, although macrophages responded less robustly than liver (95 and 73% reduction in the liver and macrophages of *Dhcr24* ASO- vs. SCR control-treated animals, respectively) (Fig. S1*C*). As in the case of liver, the major LXR target genes *Abca1* and *Abcg1* were not significantly modulated (*P* value is not significant for both, *Dhcr24* ASO vs. SCR ASO) despite increased desmosterol concentrations in plasma, liver, and macrophages (Fig. S1*D*). Taken together, these data show that while *Dhcr24*-specific ASOs reduced hepatic and macrophage expression of *Dhcr24* mRNA and protein, leading to increased levels of cellular and circulating desmosterol, they did not lead to activation of LXR target genes or suppression of SREBP target genes.

Cell Type-Specific Effect of Desmosterol in Macrophages Compared with Hepatocytes. The lack of an effect of knockdown of *Dhcr24* in the liver on LXR or SREBP target genes despite a significant increase in hepatic desmosterol raised the questions of whether desmosterol reached sufficient intracellular concentrations to be active and/or whether the desmosterol pathway is utilized in the liver. To directly compare responses of macrophages and hepatocytes to desmosterol, we evaluated the expression of *Dhcr24* and *Abca1* in plated TGEMs and *DHCR24* and *ABCA1* in HepG2 cells treated with increasing concentrations of desmosterol and the synthetic LXR ligand T0901317 (Fig. 2*A*). Whereas treatment with T0901317 resulted in an increase of *Abca1* expression in TGEMs (19.05 ± 3.86, $P < 0.01$ for 1 μM T0901317 relative to vehicle) and *ABCA1* expression in HepG2 cells (1.80 ± 0.30, $P < 0.01$ for 1 μM T0901317 relative to vehicle), this LXR target gene was up-regulated only in TGEMs (8.51 ± 1.40, $P < 0.01$ relative to vehicle) but not HepG2 cells after treatment with 10 μM desmosterol. In addition, while there was no effect of T0901317 on the suppression of the SREBP target gene *Dhcr24* in either cell type, treatment with 10 μM desmosterol resulted in a marked down-regulation of *Dhcr24* (0.19 ± 0.08, $P < 0.01$ relative to vehicle) solely in TGEMs (Fig. 2*A*).

To further explore the specific LXR- and SREBP-dependent gene responses to desmosterol, we performed qRT-PCR analysis in primary macrophages and primary hepatocytes from both mice and humans (Fig. 2 *B* and *C*). Treatment of TGEMs with 10 μM desmosterol resulted in an increase in the LXR-responsive gene *Abca1* (8.06 ± 1.80, $P < 0.05$ relative to vehicle) and a decrease in *Dhcr24* (0.19 ± 0.04, $P < 0.05$ relative to vehicle) without subsequent activation of the SREBP-responsive gene fatty acid synthase (*Fasn*), whereas it had no effect in primary mouse hepatocytes (Fig. 2*B*). In contrast, treatment of cells with the synthetic selective LXR ligand GW3965 resulted in increased levels of *Abca1* (22.77 ± 4.62, $P < 0.05$ relative to vehicle) and *Fasn* (7.13 ± 1.64, $P < 0.05$ relative to vehicle) mRNA in both macrophages and hepatocytes (5.58 ± 1.28, $P < 0.05$ and 3.64 ± 0.34, $P < 0.05$ for *Abca1* and *Fasn*, respectively) (Fig. 2*B*). The LXR and SREBP target gene expression changes induced by desmosterol and GW3965 in mouse macrophages and hepatocytes were fully recapitulated in human monocyte-derived macrophages (HMDMs) and primary hepatocytes (Fig. 2*C*). These data suggest that while desmosterol effectively leads to a dose-dependent increase in LXR target genes without inducing SREBP target genes, as is seen for synthetic selective LXR ligands in both human and mouse macrophages, these effects are largely absent in hepatocytes.

To examine possible mechanisms, we performed lipidomic analyses of TGEMs and primary hepatocytes from mice. Desmosterol was by far the most abundant LXR ligand present in both cell types in an inactivated/unstimulated state (Fig. 3*A*). In contrast, the oxysterol ligands 25-hydroxycholesterol and 27-hydroxycholesterol, implicated in regulating LXR activity based on genetic deletion of the genes encoding 24-, 25-, and 27-cholesterolhydroxylases (41), were almost exclusively found in hepatocytes, while 24(*S*)-hydroxycholesterol was not detected in either cell type (Fig. 3*B*). Evaluation of the extent to which exogenous desmosterol (10 μM) was taken up by macrophages and hepatocytes indicated a time-dependent accumulation in both cell types, with ∼30% greater uptake occurring in macrophages after 4 h (Fig. 3 *C* and *D*). Following 1 h of desmosterol loading (10 μM), TGEMs and hepatocytes were washed and fresh media lacking desmosterol were added. Cell-associated desmosterol remained constant over the next 4 h in macrophages but dropped significantly

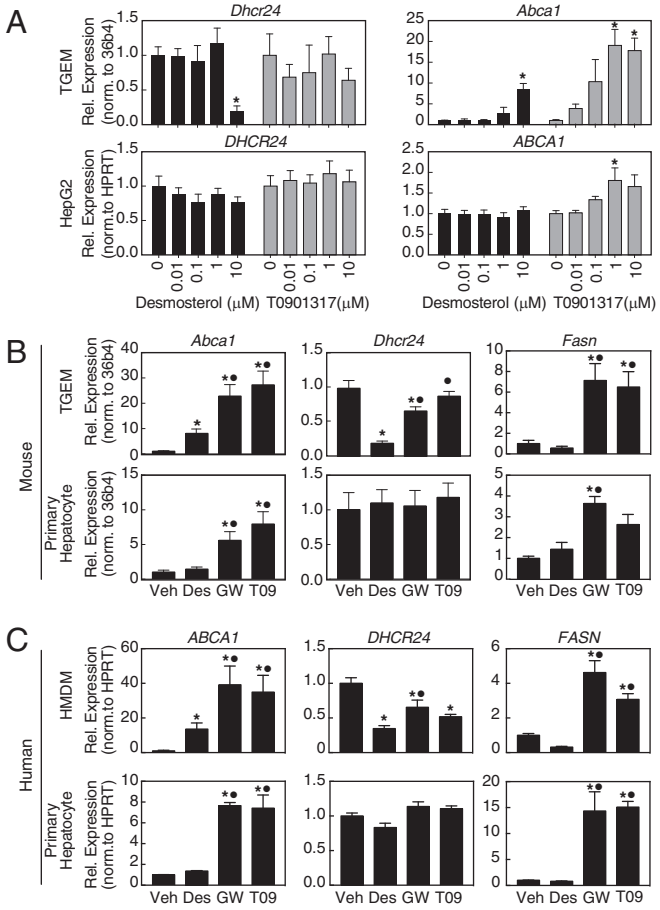

Fig. 2. LXR- and SREBP-mediated gene expression profiles in mouse and human macrophages and hepatocytes. (*A*) Dose-dependent modulation of *Dhcr24* and *ABCA1* in plated TGEMs and HepG2 cells by desmosterol and T0901317 (*$P < 0.01$). (*B*) In mouse TGEMs, desmosterol (Des; 10 μM) induces expression of *Abca1* while suppressing *Dhcr24* without affecting *Fasn*, whereas the synthetic LXR ligand GW3965 (GW; 1 μM) induces the expression of *Fasn*. In primary mouse hepatocytes, desmosterol fails to illicit changes in Abca1 and Dhcr24 while GW3965 retains its ability to activate LXR and SREBP (*$P < 0.05$ vs. Veh; •$P < 0.05$ vs. desmosterol). (*C*) The action of desmosterol (10 μM) and GW3965 (1 μM) on *ABCA1*, *DHCR24*, and *FASN* in cultured human monocyte-derived macrophages and human primary hepatocytes recapitulates the transcriptional activities observed in mouse TGEMs and hepatocytes (*$P <$ 0.05 vs. Veh; •$P < 0.05$ vs. desmosterol). HPRT, hypoxanthine-guanine phosphoribosyltransferase. Error bars represent standard errors.

by 1 h in hepatocytes (Fig. 3 *E* and *F*). Collectively, these changes suggest differences in metabolism and compartmentalization of desmosterol and oxysterols in macrophages and hepatocytes that are consistent with the observed selectivity of exogenous desmosterol in regulating LXR- and SREBP-dependent gene expression in macrophages.

Synthetic Desmosterol Mimetics Exhibit a Cell Type-Specific LXR Activation Profile Similar to Desmosterol. Appreciating the differential LXR- and SREBP target gene response in macrophages and hepatocytes of desmosterol compared with conventional LXR ligands (e.g., GW3965, T0901317), we sought synthetic compounds that might represent desmosterol mimetics. Such molecules by definition would have the functional properties of coordinately activating LXR target genes and suppressing SREBP1 and SREBP2 target genes. While the chemical structures of GW3965 and T0901317 are vastly dissimilar to desmosterol (Fig. 4*A*), DMHCA, a previously reported synthetic dissociated LXR agonist with antiatherosclerotic potential, retains much of the same desmosterol chemical backbone (24, 26, 27). In TGEMs, DMHCA not only activates LXR target genes such as *Abca1* and fails to induce *Fasn* expression, as previously reported, but also strongly represses the SREBP target gene *Dhcr24* (Fig. 4*B*). This activity profile is thus consistent with that of a desmosterol mimetic. In addition, we evaluated recently developed derivatives of DMHCA, exemplified by MePipHCA, which we reported as a dissociated LXR agonist that inhibits inflammation in models of traumatic brain injury and inflammatory bowel disease (40). Similar to DMHCA, MePipHCA not only activated the LXR target genes in macrophages but also strongly suppressed *Dhcr24* expression (Fig. 4*C*). We also observed that, in contrast to T0901317, DMHCA and MePipHCA did not cause lipid accumulation in HepG2 cells after 72-h treatment (Fig. 4*D*), consistent with a lack of an effect of DMHCA and MePipHCA on SREBP1c expression and lipid biogenesis in these cells.

Whole-Transcriptome Assessment of Desmosterol Mimetics. In view of the cell type-specific characteristics of desmosterol signaling, the similarities shared with DMHCA, especially in terms of the

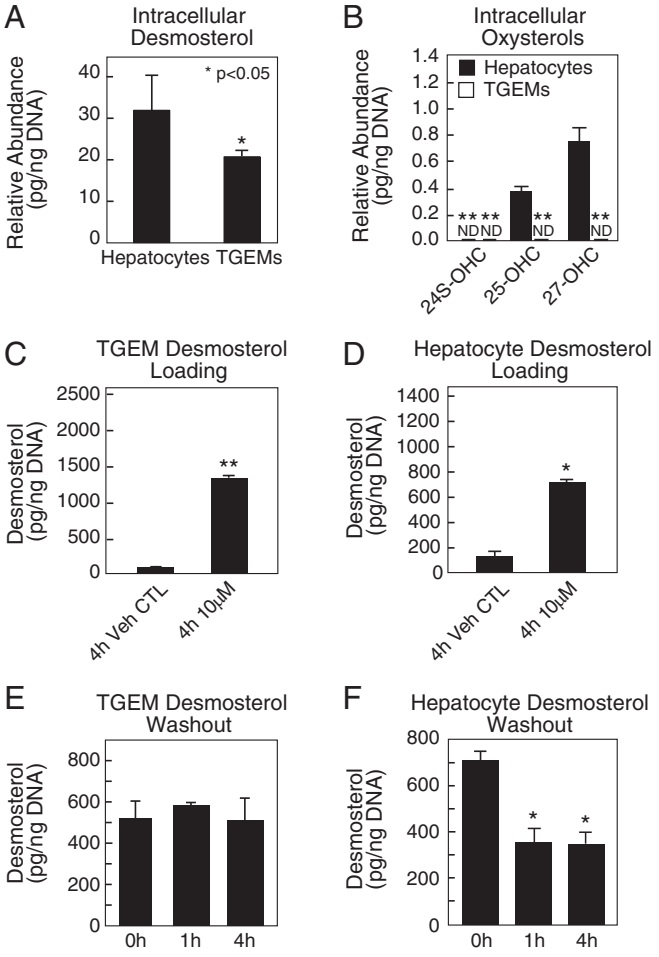

Fig. 3. Desmosterol and oxysterol levels in TGEMs and hepatocytes under steady state, loading, and washout conditions. (*A*) Desmosterol levels in TGEMs and primary hepatocytes following isolation from C57BL6/j mice (*$P < 0.05$). (*B*) 24(*S*)-, 25-, and 27-hydroxycholesterol levels in TGEMs and primary hepatocytes (ND, not detected; **$P < 0.01$). (*C* and *D*) Cellular concentrations of desmosterol in TGEMs (*C*) and hepatocytes (*D*) following incubation with 10 μM desmosterol for 4 h (*$P < 0.05$, **$P < 0.01$). (*E* and *F*) Cellular concentrations of desmosterol in TGEMs (*E*) and hepatocytes (*F*) after 1-h loading with 10 μM desmosterol, followed by washing and addition of fresh media for 1 or 4 h (*$P < 0.05$). Error bars represent standard errors.

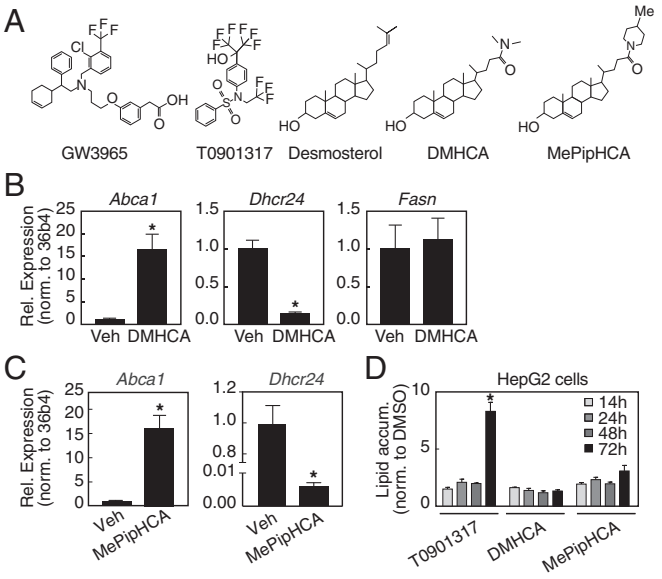

Fig. 4. DMHCA and MePipHCA have desmosterol-like activities. (*A*) Comparison of the chemical structures of GW3965, T0901317, desmosterol, DMCHA, and MePipHCA. (*B*) Effects of DMHCA (1 μM) on expression of *Abca1*, *Dhcr24*, and *Fasn* in mouse TGEMs (*$P < 0.01$ vs. Veh). (*C*) Effects of MePipHCA (1 μM) on *Abca1* and *Dhcr24* expression in mouse TGEMs (*$P < 0.01$ vs. Veh). (*D*) Effects of T0901317, DMHCA, and MePipHCA on lipid accumulation in HepG2 cells. *$P < 0.05$ vs. DMSO. Error bars represent standard errors.

dissociation of LXR- and SREBP-pathway regulation, and the promise of the structurally related mimetic MePipHCA, we conducted an unbiased, whole-transcriptome comparison of these ligands with the conventional LXR ligands GW3965 and T0901317 using RNA-sequencing (RNA-seq) analysis. We began by treating plated TGEMs and mouse primary hepatocytes with desmosterol (10 μM), DMHCA (1 μM), MePipHCA (1 μM), GW3965 (1 μM), and T0901317 (1 μM). Representative scatter plots show that while treatment with desmosterol, DMHCA, or T0901317 leads to a robust LXR response in TGEMs, the overall LXR response is absent in hepatocytes except after treatment with T0901317 (Fig. 5*A*). Heat maps of individual genes from key LXR and SREBP pathways illustrate that while all compounds tested in TGEMs induce *Abca1* expression (LXR-responsive gene), desmosterol, DMHCA, and MePipHCA repress SREBP-responsive genes (*Dhcr24*, *Hmgcr*, and *Ldlr*) while GW3965 and T0901317 activate *Fasn* and *Srebf1* (Fig. 5*B*). In mouse primary hepatocytes, only GW3965 and T0901317 retain the expected LXR activities and activate SREBP1c target genes such as *Fasn*. Gene ontology (GO) term analysis of specific up- and down-regulated gene pathways reinforced the LXR-activating effect of all compounds in TGEMs and the combined LXR- and SREBP1c-activating effect of GW3965 and T0901317 in both TGEMs and hepatocytes (Fig. 5*C*). Notably, the SREBP-mediated pathways noted by the GO terms "cholesterol metabolic process" and "sterol biosynthetic process" are markedly suppressed by desmosterol, DMHCA, and MePipHCA in macrophages (Fig. 5*C*). In principal component analysis (PCA) performed on the differentially expressed genes (up and down) in both TGEMs (*Left*) and primary hepatocytes (*Right*), the conventional ligands GW3965 and T0901317 cluster tightly together, as do desmosterol and DMHCA, with MePipHCA assorting itself distinctly along the first two eigenvectors (Fig. 5*D*). The divergence of MePipHCA for up-regulated genes is partly driven by its activation of several genes that have functional annotations associated with the "response to unfolded protein" pathway in GO term analysis, including Atf4, Chac1, Ddit3, and Chop (Fig. S2*A*). Of note, this pathway is also activated by 25-hydroxycholesterol in macrophages (42).

We observed similar differences in the transcriptional responses of macrophages and hepatocytes in our unbiased, whole-transcriptome RNA-seq analysis of human cells. First, we compared the global response of up- and down-regulated genes in response to these ligands in both HMDMs and human primary hepatocytes (Fig. 6*A*). Notably, and similar to our studies in mouse cells, desmosterol and DMHCA activated LXR target genes and blunted SREBP1 and SREBP2 target genes in HMDMs but exhibited minimal effects on these genes in primary hepatocytes. In contrast, T0901317 activated LXR and SREBP1 target genes in both cell types. The most significant transcriptional pathways up- and down-regulated by these treatments in HMDMs and human primary hepatocytes are relatively unchanged from mouse, with the coordinated activation of reverse cholesterol transport and suppression of cholesterol and triglyceride biosynthetic pathways observed in macrophages (Fig. 6*B*). This pathway analysis is supported on the individual gene level (Fig. 6*C*). In addition, HMDMs from five individual patients with varying degrees of coronary atherosclerosis and comorbid chronic diseases were treated with desmosterol, DMHCA, and T0901317. While the range of transcriptional responses to these ligands likely highlights the influence of natural genetic variation, all HMDMs showed robust increases in LXR-mediated genes (*ABCA1*, *ABCG1*) when treated with desmosterol, DMHCA, and T0901317. T0901317 activated SREBP target genes (*SCD*, *FASN*), while these genes were suppressed or unchanged in response to desmosterol or DMHCA, respectively. Most apparent here is the global similarity of DMHCA to the natural oxysterol desmosterol in regard to LXR and SREBP transcriptional control, and their differences with the conventional LXR agonist T0901317 (Fig. 6*C*). While desmosterol, DMHCA, and MePipHCA activate LXR-mediated pathways and suppress SREBP-mediated pathways in macrophages of mice and humans, this response is absent or blunted in primary hepatocytes. Conversely, GW3965 and T0901317 remain potent activators of LXR-pathway genes in both cell types while activating SREBP-responsive genes in tandem. MePipHCA also activated a subset of genes associated with the unfolded protein response, as observed in mouse macrophages (Fig. S2*B*).

While the vast majority of genes that were up- and down-regulated by desmosterol, DMHCA, and T0901317 were shared in mouse and human macrophages, we also noted certain genes that were differentially regulated (Fig. 6*D*). While the roles of many of these genes in lipid homeostasis and regulation of inflammation remain unappreciated, we did observe differences in key genes such as the nuclear receptor LXRα (*NR1H3*) and retinoic acid receptor (*RARA*), both differentially induced in HMDMs, and several regulators of lipid metabolism such as fatty acid desaturase (*FADS1*), 7-dehydrocholesterol reductase (*DHCR7*), and farnesyl-diphosphate farnyltransferase (*FDFT1*), all suppressed in HMDMs compared with mouse TGEMs.

The Macrophage-Specific Induction of LXR-Responsive Genes Without Potentiation of SREBP Pathways with Synthetic Desmosterol Mimetics Is Recapitulated in Vivo. We then sought to examine if the cell type-specific effects observed in plated macrophages and hepatocytes in response to desmosterol and desmosterol mimetics (DMHCA and MePipHCA) were recapitulated in an in vivo model. We treated mice with thioglycollate by i.p. injection 4 d before treatment with compounds to elicit macrophage accumulation in the peritoneum. DMHCA, MePipHCA, and T0901317 (50 mg/kg) were then given by i.p. injection 6 and 16 h before peritoneal macrophages, and whole liver was isolated and prepared for gene expression analysis. Gene expression of the LXR-responsive gene *Abca1* was robustly induced in peritoneal macrophages at 6 h by T0901317, DMHCA, and MePipHCA, whereas only T0901317 induced a coordinate response in *Abcg5* in the liver (Fig. 7*A*). The LXR-activating effect

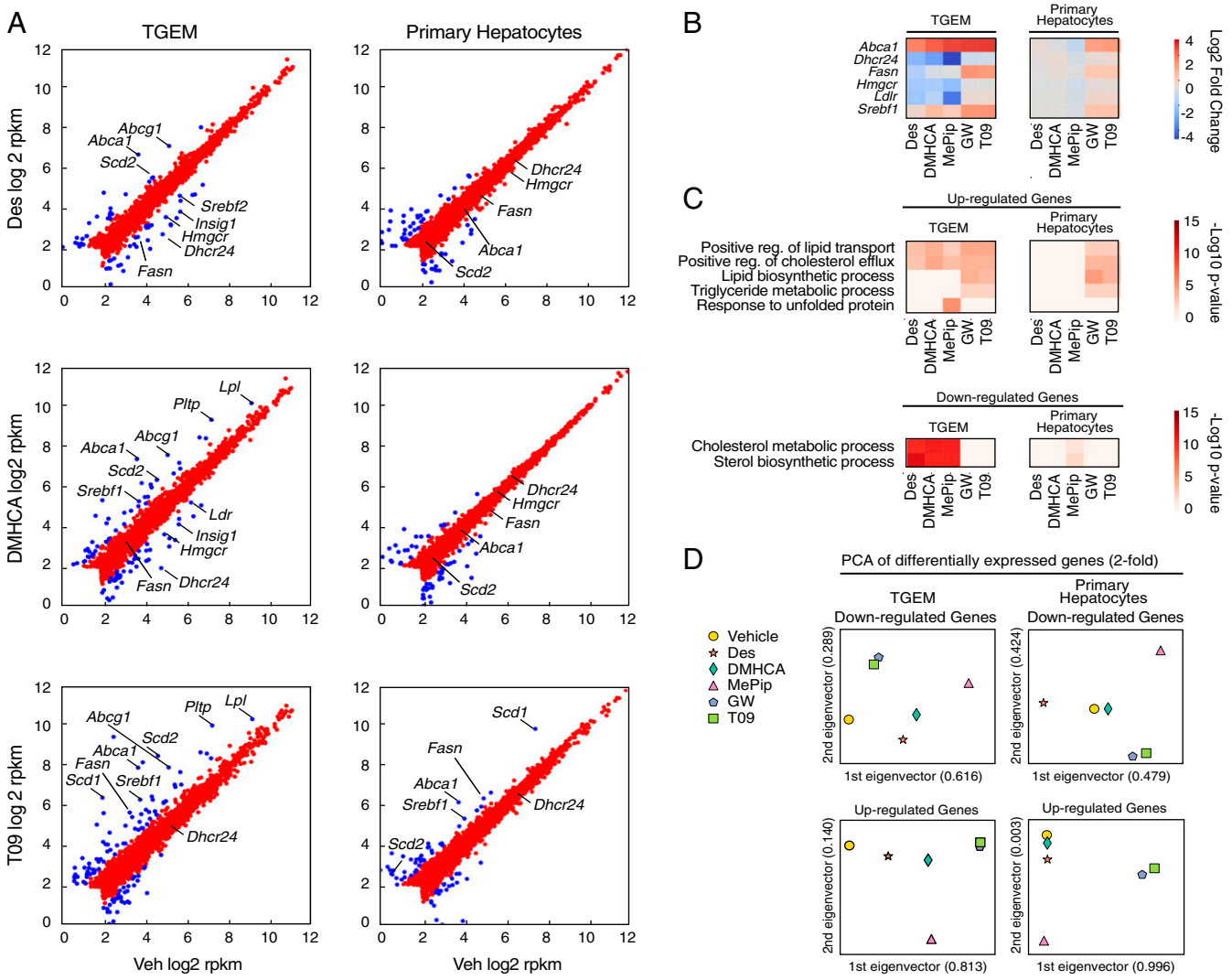

Fig. 5. Whole-transcriptome RNA-sequencing assessment of mouse TGEMs and primary hepatocytes. (*A*) Scatter plots for up- and down-regulated genes in TGEMs ($n = 3$ per treatment) and primary hepatocytes ($n = 2$ per treatment) after exposure to desmosterol (10 μM), DMHCA (1 μM), and T0901317 (1 μM). Key LXR and SREBP target genes are highlighted. Genes noted in blue have twofold changes versus vehicle with false discovery rate (FDR) <0.05. rpkm, reads per kilobase of transcript per million mapped reads. (*B*) Heat map for key genes illustrating logtwofold change compared with vehicle in TGEMs and primary hepatocytes. (*C*) GO term analysis of up-regulated and down-regulated genes in response to various ligands. (*D*) PCA for all differentially expressed genes with twofold changes and FDR <0.05 versus vehicle.

for DMHCA and MePipHCA was attenuated at 16 h in macrophages, though remained strong for T0901317 in both tissues. Mirroring what we had observed in in vitro studies, treatment with T0901317 led to the induction of SREBP-responsive genes, illustrated here by *Fasn*, in both macrophages and liver, while DMHCA and MePipHCA did not induce *Fasn* in either tissue.

Although responses to DMHCA and MePipHCA were minimal or absent in intact liver, it was of interest to determine whether Kupffer cells, the resident macrophage population of the liver, exhibited similar responses to those observed in elicited peritoneal macrophages. To address this question, we treated mice with vehicle, DMHCA, or T0901317 by i.p. injection, and 12 h following injection Kupffer cells were purified by fluorescence-activated cell sorting with target cells identified by $CD45^+F4/80^+CD11b^{int}Tim4^+CD146^-CD31^-$ (Fig. S3). As in the case of peritoneal macrophages, DMHCA was shown to selectively activate LXR-responsive genes in Kupffer cells (*Abca1*) but not whole liver (*Abcg5*) (Fig. 7*B*). DMHCA had no effect on the SREBP1-responsive gene *Fas* in either Kupffer cells or intact liver compared with T0901317, and modestly repressed *Hmgcr* in Kupffer cells (Fig. S3). Of note, DMHCA activated *Scd2* in Kupffer cells but not intact liver, consistent with the ability of *Scd2* to be activated independently by the LXR and SREBP1 pathways (33). These results indicate that these sterol-based synthetic LXR agonists (DMHCA and MePipHCA) appear to act preferentially in macrophages (and Kupffer cells) compared with hepatocytes in vivo and, unlike T0901317, without potentiating SREBP1-responsive genes at the level of intact liver.

Discussion

Despite their key roles at the intersection of lipid metabolism and inflammation, the promise of LXRs as pharmacologic targets for the prevention and treatment of atherosclerotic heart disease has been limited by the difficulty of decoupling beneficial effects from activation of SREBP1-dependent pathways. Development of selective LXR modulators has been challenging in part because there are few evident rationale approaches for achieving this goal. A leading strategy has been to synthesize molecules that preferentially activate LXRβ, based on evidence

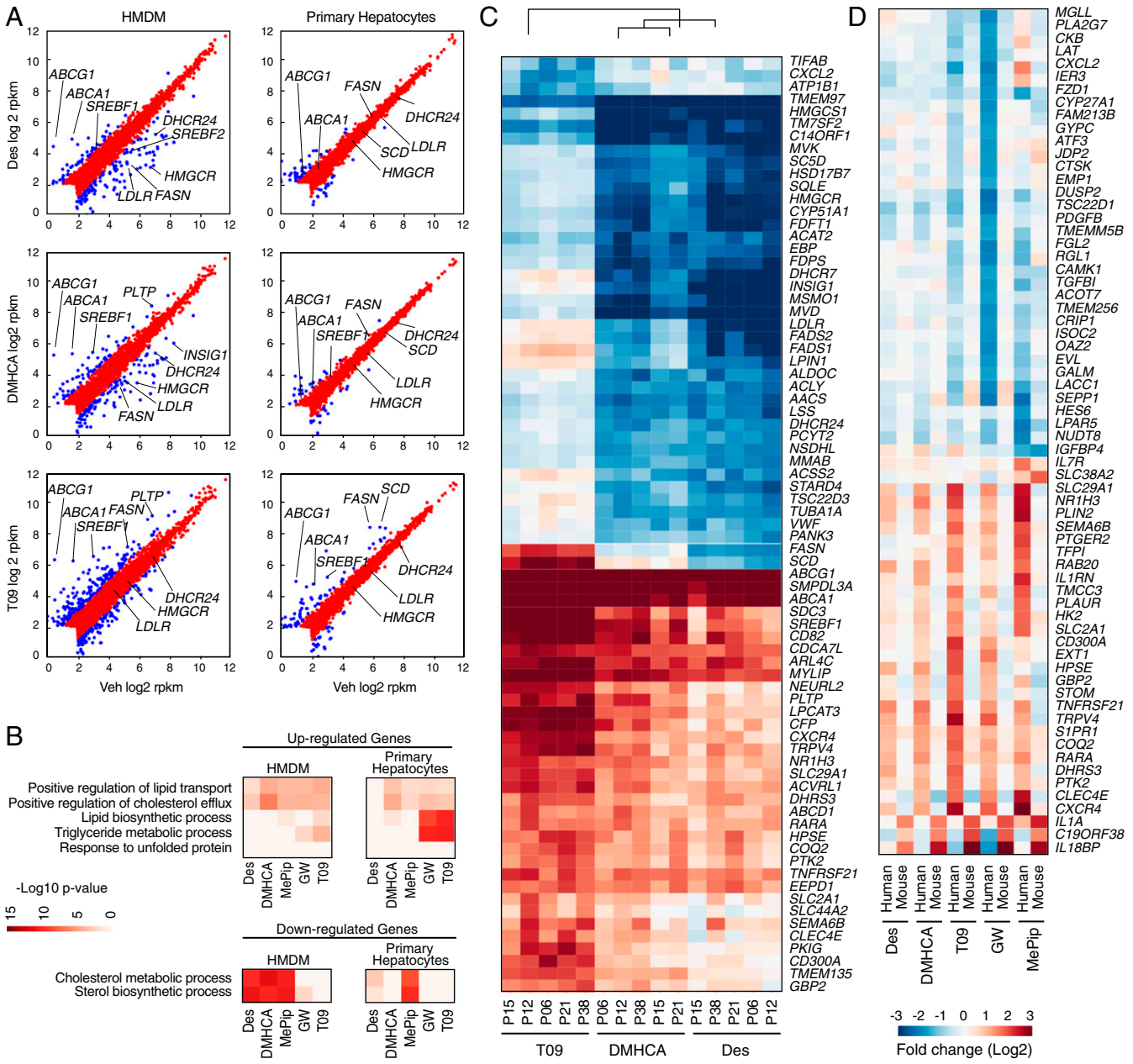

Fig. 6. RNA-seq analysis reveals an overall conserved transcriptional response to LXR ligands in human macrophages and primary hepatocytes in mice; however, key differences remain. (*A*) Scatter plots for up- and down-regulated genes in HMDMs and primary hepatocytes after exposure to desmosterol (10 μM), DMHCA (1 μM), and T0901317 (1 μM). (*B*) GO term analysis of up-regulated and down-regulated genes in response to various ligands. (*C*) Heat map illustrating a shared global gene expression pattern in individual HMDMs ($n = 5$) in response to desmosterol and DMHCA that is divergent from T0901317. (*D*) Heat map of genes that are differentially regulated in macrophages of mice and humans.

for a dominant role of LXRα in driving SREBP1c expression and fatty acid biosynthesis in mouse liver (9, 19, 42, 43). However, a recent evaluation of a prototypic LXRβ-selective synthetic ligand demonstrated that in addition to induction of LXR target genes in human blood cells and inhibition of atherosclerosis in mouse models, it retained the ability to increase circulating triglyceride levels and hepatic triglycerides in human subjects (44).

Here we have explored an alternative strategy that is based on the observation that most or all physiologic LXR agonists are also inhibitors of SREBP processing, either by binding to INSIGs (e.g., oxysterols) or SCAP (desmosterol). In contrast to synthetic agonists that selectively target LXRs, such endogenous ligands would be expected to activate genes involved in reduction of cellular cholesterol but have an attenuated effect on fatty acid biosynthesis due to inhibitory effects on processing of SREBP1c. We thus sought to test the hypothesis that raising endogenous levels of LXR agonists or mimicking their activity would have these effects.

Our initial in vivo approach was to increase intracellular concentrations of desmosterol by specifically reducing the activity of DHCR24 using antisense oligonucleotide technology. Unexpectedly, despite a marked elevation in hepatic and circulating desmosterol levels after treatment with *Dhcr24*-specific ASOs, we failed to observe concomitant activation of key LXR-responsive genes in the liver or macrophages. One possible interpretation of this result is that, while significantly elevated,

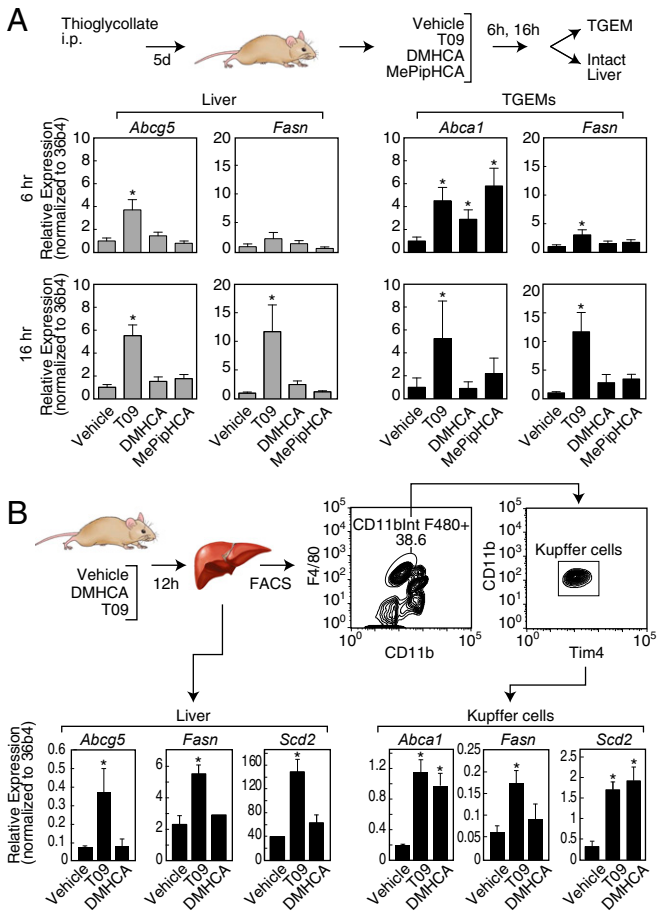

Fig. 7. Cell type-specific effects on LXR- and SREBP-responsive genes in vivo. (*A*) Gene expression profiling of LXR and SREBP target genes in mouse liver and peritoneal macrophages (TGEMs) 6 and 16 h after i.p. administration of T0901317 (T09), DMHCA, and MePipHCA compared with vehicle (M-Pyrol) (*$P < 0.05$ vs. Veh). (*B*) Gene expression profiles of *Abca1*, *Abcg5*, and *Fasn* of isolated Kupffer cells and whole liver in mice treated with i.p. DMHCA, T0901317 (T09), or vehicle for 12 h (*$P < 0.05$ vs. Veh). Error bars represent standard errors.

desmosterol did not reach intracellular concentrations required to activate LXRs. This hypothesis was supported by our observation that 10 μM desmosterol significantly elevated LXR target genes in TGEMs but not 1 μM desmosterol (Fig. 2*A*). In addition, serum desmosterol levels of *Dhcr24* ASO-treated mice were less than 20% of those observed in human subjects treated with triparanol or in the rare genetic disease of desmosterolosis (39, 45, 46). We conclude that raising endogenous desmosterol levels by reducing *Dhcr24* expression using ASOs is unlikely to be an effective strategy for activation of LXRs in vivo.

Given the inability to modulate the LXR axis by increasing endogenous desmosterol concentrations with *Dhcr24* ASO, we sought to specifically assess the desmosterol pathway in hepatocytes. Unexpectedly, we observed that concentrations of desmosterol that effectively activated LXR-responsive genes and suppressed SREBP-responsive genes in macrophages had little or no effect on these genes in mouse and human hepatocytes. Thus, these studies provide evidence for a cell-autonomous mechanism enabling cell-specific discrimination of an endogenous LXR ligand that confers selective activation of LXR target genes in macrophages.

Based on these findings, we characterized DMHCA, an empirically developed LXR agonist that exhibits antiatherosclerotic activity without causing substantial hypertriglyceridemia in mice (24). Importantly, unlike conventional LXR agonists such as GW3965 and T0901317, DMHCA is structurally related to desmosterol, raising the possibility that it functions as a desmosterol mimetic. Consistent with this possibility, DMHCA coordinately induced LXR target genes and repressed both SREBP1 and SREBP2 target genes. We therefore evaluated a series of derivatives capable of activating LXRs in transient transfection assays, the most potent of which was MePipHCA. This result provides evidence of the possibility of improving the physicochemical properties of this class of compounds for pharmaceutical use.

Genome-wide comparisons of desmosterol, DMHCA, MePipHCA, GW3965, and T0901317 in mouse and human macrophages and hepatocytes strongly support the preferential activities of desmosterol and desmosterol mimetics in macrophages and demonstrate that they coordinately regulate the LXR and SREBP pathways in these cells. Desmosterol, DMHCA, and MePipHCA regulated a highly overlapping set of genes, with DMHCA and MePipHCA exhibiting greater potency. Comparisons of the responses of mouse and human macrophages also indicated a high degree of similarity at the level of genes involved in cholesterol homeostasis. A relatively small number of genes exhibited species-specific differences in responses, primarily in human monocyte-derived macrophages, which are at this point of uncertain significance. There was relatively little individual variation in responses of the core set of LXR target genes involved in cholesterol homeostasis among the small set of human monocyte-derived macrophages that were evaluated. Importantly, the macrophage-selective activities of DMHCA and MePipHCA were observed in vivo.

In addition to regulating the LXR/SREBP pathways, desmosterol was previously shown to inhibit inflammatory responses in macrophages, consistent with the actions of other LXR agonists (33). Although not evaluated for antiinflammatory effects in these studies, we recently reported that MePipHCA significantly reduced disease severity and inflammatory markers in models of inflammatory bowel disease and traumatic brain injury without causing lipid accumulation in the liver (40). A limitation of the current synthetic desmosterol mimetics is a relatively poor pharmacokinetic profile, requiring large doses for in vivo efficacy. Therefore, it is likely that substantial additional effort will be required to develop more drug-like molecules.

A major new and exciting question regards the basis for cell-specific discrimination of desmosterol that confers preferential activity in macrophages. It is unlikely to be simple conversion of desmosterol to cholesterol or another LXR agonist, because similar activities were observed for the synthetic agonists DMHCA and MePipHCA. A cell-autonomous basis for this discrimination is strongly supported by the finding that Kupffer cells in the liver robustly respond to DMHCA, while surrounding hepatocytes do not. Lipidomic studies indicate that desmosterol is by far the most abundant LXR ligand in both macrophages and hepatocytes, while 25-hydroxycholesterol and 27-hydroxycholesterol are preferentially found in hepatocytes. Notably, macrophages took up and retained more exogenous desmosterol than hepatocytes. Collectively, these findings suggest a hepatocyte-specific mechanism that distinguishes between desmosterol/desmosterol mimetics and oxysterols, given the genetic evidence that 24-hydroxycholesterol, 25-hydroxycholesterol, and 27-hydroxycholesterol are endogenous agonists of LXRs in the liver (41). We speculate that proteins involved in the intracellular transport of desmosterol/desmosterol mimetics restrict their access to SCAP and SREBPs in hepatocytes but not macrophages. Further understanding of the mechanism underlying differential actions of desmosterol in macrophages and hepatocytes thus remains an important future goal.

Materials and Methods

Reagents. Desmosterol was purchased from Avanti Polar Lipids. DMHCA was resynthesized internally, along with the design and synthesis of MePipHCA.

Mevastatin, mevalonolactone, and M-Pyrol were purchased from Sigma-Aldrich. GW3965 and T0901317 were purchased from Cayman Chemical.

Antisense Oligonucleotides. All antisense oligonucleotides used for these studies were designed by Ionis Pharmaceuticals to hybridize to the sequence spanning mouse DHCR24 mRNA. The scrambled control ASO is a chemistry control ASO that has the same length and chemical make-up as the DHCR24-specific ASO, and is not expected to hybridize to any mRNA sequence. For in vitro cell studies, ASOs were transfected into cells using Cytofectin (Genlantis) at 50 nM final concentration. For animal studies, ASOs were delivered in sterile saline at either 20 mg ASO per kg animal weight by twice-weekly i.p. injections or at 100 mg/kg delivered s.c.

Animals. All animal studies were approved by the University of California, San Diego Institutional Animal Care and Use Committee. Adult male C57BL/6 mice were acquired from Charles River Laboratories. Mice were maintained in an institutional animal care and use committee-approved animal facility with a standard light–dark cycle and fed standard laboratory chow.

Thioglycollate-Elicited Macrophage Generation. Peritoneal macrophages were harvested 4 d after i.p. injection of thioglycollate (refer to *Supporting Information* for additional details).

Cell Culture. Thioglycollate-elicited macrophages and HepG2 cells were maintained in RPMI-1640 with 10% FBS and 100 U/mL penicillin/streptomycin (Cellgro/Corning). Primary mouse hepatocytes were prepared as described and maintained in HepatoZYME medium (Gibco) with 10% FBS, 1% L-glutamine, and 1% penicillin/streptomycin (refer to *Supporting Information* for additional details).

Isolation and Culture of Human Monocyte-Derived Macrophages. Human monocyte-derived macrophages were obtained under research protocol (UCSD IRB-12-0902) approved by the University of California, San Diego Institutional Review Board. Following informed consent, de-identified blood was obtained from patients undergoing cardiac catheterization from the arterial sheath after access achieved but prior to any administration of contrast agent. Human macrophages were prepared from $CD14^+$ peripheral blood mononuclear cells (PBMCs) isolated from human blood by incubating in RPMI-1640 + 10% FBS supplemented with penicillin/streptomycin and 50 ng/mL recombinant human macrophage colony-stimulating factor (R&D Systems) (refer to *Supporting Information* for additional details).

In Vivo Injection of LXR Agonists and Purification of Kupffer Cells. Mice were treated by i.p. injection with 50 mg/kg of DMHCA or T0901317 dissolved in 50:50 ethanol and M-Pyrol at a concentration of 50 mg/mL. Twelve hours later, mice were humanely euthanized by exposure to CO_2; whole-liver pieces were saved and liver nonparenchymal cells were processed for fluorescence-activated cell sorting of Kupffer cells, with modifications from published methodology (47, 48) (refer to *Supporting Information* for additional details).

RNA Isolation and Quantitative PCR. Total RNA was isolated with TRIzol reagent (Life Technologies) and Direct-zol RNA spin columns (Zymo Research). Total RNA was used for either first-strand cDNA synthesis with SuperScript III (Life Technologies) or RNA-seq library preparation. Real-time PCRs were prepared in 96-well plates using iTaq SYBR Green Supermix (Bio-Rad) and performed on the StepOnePlus Quantitative PCR platform (Life Technologies) (refer to *Supporting Information* for additional details).

RNA-Sequencing Library Preparation. Please see *Supporting Information* for details. Briefly, polyA RNA was used for first-strand cDNA synthesis. Second-strand synthesis was carried out using deoxy-UTP. Following end repair, the product was then incubated with EDAC Sera-Mag SpeedBeads (GE Healthcare) and eluted with manufacturer-supplied elution buffer (Zymo Research). This was followed by dA tailing, unique barcode adapter ligation, and second-strand digestion with UDG (Enzymatics). PCR amplification was performed by 12 to 15 cycles and size-selected for 223 to 375 bp after separating on a 10% Tris borate ethylenediaminetetraacetic acid buffer (TBE) gel (Life Technologies). The library was purified from the gel slice and single-end–sequenced on a HiSeq 2000 instrument (Illumina).

Plasma Analysis and Lipid Measurements. Plasma, liver, and TGEMs were processed at the University of Texas Southwestern Medical Center for oxysterol and lipid metabolite analysis by LC-MS as previously described in full (www.lipidmaps.org/protocols/index.html).

Western Blot Analyses. Protein extracts were fractionated using a 4 to 12% Bis-Tris NuPAGE (Invitrogen) gel and blotted onto an Immobilon-P PVDF membrane (EMD Millipore). Membranes were incubated with primary antibody against mouse DHCR24 (Cell Signaling Technology) or beta-actin (Santa Cruz Biotechnology) overnight at 4 °C followed by a secondary antibody conjugated to Alexa Fluor 680 (Molecular Probes) or IRDye 800 (Rockland). Membranes were then imaged using the LI-COR Odyssey. Please see *Supporting Information* for details.

HCS LipidTOX Neutral Lipid Stain Assay. HepG2 cells were plated in 384-well plates at a density of 5,000 cells per well. The cells were treated with compounds at 1 μM concentration for different time points as indicated, followed by fixing with 3% formaldehyde and staining with HCS LipidTOX neutral lipid stain (H34475; Invitrogen) according to the manufacturer's protocol. The lipid content was quantified and analyzed by Cellomics high-content imaging system and software.

Data Analysis. Experimental values are presented as the means of replicate experiments ±SE. Aside from the RNA-seq experiments, comparisons among groups were made using analysis of variance followed by Student's *t* test for pairwise comparison with correction for multiple comparisons. using Prism 7.0 software (GraphPad). Statistical significance was defined as $P < 0.05$. Please see *Supporting Information* for details regarding RNA-seq analysis.

ACKNOWLEDGMENTS. We appreciate the generosity of the research volunteers, who made parts of this study possible. We thank Leslie Van Ael for assistance with preparation of figures. These studies were supported by NIH Grants HL088093, GM085764, DK063491 (all to C.K.G.), and HL20948 (to J.G.M.). C.K.G. is also supported by the Ben and Wanda Hildyard Chair in Hereditary Diseases. E.D.M. is supported by NIH/NCATS Clinical Translational Science Awards 5KL2TR001112 and 5UL1TR001114 to the Scripps Translational Science Institute. S.Y. is supported by Crohn's and Colitis Foundation of America Research Fellowship Award 368561. T.D.T. was supported by the National Cancer Institute of the National Institutes of Health under Award T32CA009523. J.S.S. was supported by American Heart Association Fellowship 16PRE30980030 and NIH Predoctoral Training Grant 5T32DK007541. C.K.G. and S.T. are supported by a Fondation Leducq Transaltlantic Network grant.

1. Benjamin EJ, et al.; American Heart Association Statistics Committee; Stroke Statistics Subcommittee (2017) Heart disease and stroke statistics—2017 update: A report from the American Heart Association. *Circulation* 135:e146–e603.
2. World Health Organization (2014) *Global Status Report on Noncommunicable Diseases 2014* (WHO, Geneva).
3. Gotto AM, Jr, Moon JE (2013) Pharmacotherapies for lipid modification: Beyond the statins. *Nat Rev Cardiol* 10:560–570.
4. Stone NJ, et al.; American College of Cardiology/American Heart Association Task Force on Practice Guidelines (2014) 2013 ACC/AHA guideline on the treatment of blood cholesterol to reduce atherosclerotic cardiovascular risk in adults: A report of the American College of Cardiology/American Heart Association Task Force on Practice Guidelines. *Circulation* 129(25, Suppl 2):S1–S45.
5. Hansson GK, Robertson A-KL, Söderberg-Nauclér C (2006) Inflammation and atherosclerosis. *Annu Rev Pathol* 1:297–329.
6. Libby P (2012) Inflammation in atherosclerosis. *Arterioscler Thromb Vasc Biol* 32:2045–2051.
7. McLaren JE, Michael DR, Ashlin TG, Ramji DP (2011) Cytokines, macrophage lipid metabolism and foam cells: Implications for cardiovascular disease therapy. *Prog Lipid Res* 50:331–347.
8. Moore KJ, Tabas I (2011) Macrophages in the pathogenesis of atherosclerosis. *Cell* 145:341–355.
9. Calkin AC, Tontonoz P (2012) Transcriptional integration of metabolism by the nuclear sterol-activated receptors LXR and FXR. *Nat Rev Mol Cell Biol* 13:213–224.
10. Im S-S, Osborne TF (2011) Liver X receptors in atherosclerosis and inflammation. *Circ Res* 108:996–1001.
11. Parikh N, Frishman WH (2010) Liver X receptors: A potential therapeutic target for modulating the atherosclerotic process. *Cardiol Rev* 18:269–274.
12. Costet P, Luo Y, Wang N, Tall AR (2000) Sterol-dependent transactivation of the ABC1 promoter by the liver X receptor/retinoid X receptor. *J Biol Chem* 275: 28240–28245.
13. Venkateswaran A, et al. (2000) Control of cellular cholesterol efflux by the nuclear oxysterol receptor LXR alpha. *Proc Natl Acad Sci USA* 97:12097–12102.
14. Joseph SB, Castrillo A, Laffitte BA, Mangelsdorf DJ, Tontonoz P (2003) Reciprocal regulation of inflammation and lipid metabolism by liver X receptors. *Nat Med* 9: 213–219.
15. Naik SU, et al. (2006) Pharmacological activation of liver X receptors promotes reverse cholesterol transport in vivo. *Circulation* 113:90–97.

16. Repa JJ, et al. (2000) Regulation of absorption and ABC1-mediated efflux of cholesterol by RXR heterodimers. *Science* 289:1524–1529.
17. Levin N, et al. (2005) Macrophage liver X receptor is required for antiatherogenic activity of LXR agonists. *Arterioscler Thromb Vasc Biol* 25:135–142.
18. Tangirala RK, et al. (2002) Identification of macrophage liver X receptors as inhibitors of atherosclerosis. *Proc Natl Acad Sci USA* 99:11896–11901.
19. Bradley MN, et al. (2007) Ligand activation of LXR beta reverses atherosclerosis and cellular cholesterol overload in mice lacking LXR alpha and apoE. *J Clin Invest* 117: 2337–2346.
20. Joseph SB, et al. (2002) Synthetic LXR ligand inhibits the development of atherosclerosis in mice. *Proc Natl Acad Sci USA* 99:7604–7609.
21. Terasaka N, et al. (2003) T-0901317, a synthetic liver X receptor ligand, inhibits development of atherosclerosis in LDL receptor-deficient mice. *FEBS Lett* 536:6–11.
22. Grefhorst A, et al. (2002) Stimulation of lipogenesis by pharmacological activation of the liver X receptor leads to production of large, triglyceride-rich very low density lipoprotein particles. *J Biol Chem* 277:34182–34190.
23. Schultz JR, et al. (2000) Role of LXRs in control of lipogenesis. *Genes Dev* 14: 2831–2838.
24. Kratzer A, et al. (2009) Synthetic LXR agonist attenuates plaque formation in apoE-/- mice without inducing liver steatosis and hypertriglyceridemia. *J Lipid Res* 50: 312–326.
25. Peng D, et al. (2008) Antiatherosclerotic effects of a novel synthetic tissue-selective steroidal liver X receptor agonist in low-density lipoprotein receptor-deficient mice. *J Pharmacol Exp Ther* 327:332–342.
26. Pfeifer T, et al. (2011) Synthetic LXR agonist suppresses endogenous cholesterol biosynthesis and efficiently lowers plasma cholesterol. *Curr Pharm Biotechnol* 12: 285–292.
27. Quinet EM, et al. (2004) Gene-selective modulation by a synthetic oxysterol ligand of the liver X receptor. *J Lipid Res* 45:1929–1942.
28. Janowski BA, Willy PJ, Devi TR, Falck JR, Mangelsdorf DJ (1996) An oxysterol signalling pathway mediated by the nuclear receptor LXR alpha. *Nature* 383:728–731.
29. Lehmann JM, et al. (1997) Activation of the nuclear receptor LXR by oxysterols defines a new hormone response pathway. *J Biol Chem* 272:3137–3140.
30. Yang C, et al. (2006) Sterol intermediates from cholesterol biosynthetic pathway as liver X receptor ligands. *J Biol Chem* 281:27816–27826.
31. Radhakrishnan A, Sun L-P, Kwon HJ, Brown MS, Goldstein JL (2004) Direct binding of cholesterol to the purified membrane region of SCAP: Mechanism for a sterol-sensing domain. *Mol Cell* 15:259–268.
32. Brown MS, Goldstein JL (2009) Cholesterol feedback: From Schoenheimer's bottle to Scap's MELADL. *J Lipid Res* 50(Suppl):S15–S27.
33. Spann NJ, et al. (2012) Regulated accumulation of desmosterol integrates macrophage lipid metabolism and inflammatory responses. *Cell* 151:138–152.
34. Avigan J, Steinberg D, Thompson MJ, Mosettig E (1960) Mechanism of action of MER-29, an inhibitor of cholesterol biosynthesis. *Biochem Biophys Res Commun* 2:63–65.
35. Steinberg D, Avigan J, Feigelson EB (1961) Effects of triparanol (Mer-29) on cholesterol biosynthesis and on blood sterol levels in man. *J Clin Invest* 40:884–893.
36. Kirby TJ (1967) Cataracts produced by triparanol (MER/29). *Trans Am Ophthalmol Soc* 65:494–543.
37. Laughlin RC, Carey TF (1962) Cataracts in patients treated with triparanol. *JAMA* 181: 339–340.
38. Winkelmann RK, Perry HO, Achor RW, Kirby TJ (1963) Cutaneous syndromes produced as side effects of triparanol therapy. *Arch Dermatol* 87:372–377.
39. Schaaf CP, et al. (2011) Desmosterolosis—Phenotypic and molecular characterization of a third case and review of the literature. *Am J Med Genet A* 155:1597–1604.
40. Yu S, et al. (2016) Dissociated sterol-based liver X receptor agonists as therapeutics for chronic inflammatory diseases. *FASEB J* 30:2570–2579.
41. Chen W, Chen G, Head DL, Mangelsdorf DJ, Russell DW (2007) Enzymatic reduction of oxysterols impairs LXR signaling in cultured cells and the livers of mice. *Cell Metab* 5: 73–79.
42. Lund EG, et al. (2006) Different roles of liver X receptor alpha and beta in lipid metabolism: Effects of an alpha-selective and a dual agonist in mice deficient in each subtype. *Biochem Pharmacol* 71:453–463.
43. Quinet EM, et al. (2006) Liver X receptor (LXR)-beta regulation in LXRalpha-deficient mice: Implications for therapeutic targeting. *Mol Pharmacol* 70:1340–1349.
44. Kirchgessner TG, et al. (2016) Beneficial and adverse effects of an LXR agonist on human lipid and lipoprotein metabolism and circulating neutrophils. *Cell Metab* 24: 223–233.
45. Andersson HC, Kratz L, Kelley R (2002) Desmosterolosis presenting with multiple congenital anomalies and profound developmental delay. *Am J Med Genet* 113: 315–319.
46. FitzPatrick DR, et al. (1998) Clinical phenotype of desmosterolosis. *Am J Med Genet* 75:145–152.
47. Seki E, et al. (2007) TLR4 enhances TGF-beta signaling and hepatic fibrosis. *Nat Med* 13:1324–1332.
48. Mederacke I, Dapito DH, Affò S, Uchinami H, Schwabe RF (2015) High-yield and high-purity isolation of hepatic stellate cells from normal and fibrotic mouse livers. *Nat Protoc* 10:305–315.